NANO MICRO small

DNA Origami

A DNA Origami Nanorobot Controlled by Nucleic Acid Hybridization

*Emanuela Torelli, Monica Marini, Sabrina Palmano, Luca Piantanida, Cesare Polano, Alice Scarpellini, Marco Lazzarino, and Giuseppe Firrao**

***A** prototype for a DNA origami nanorobot has been designed, produced and tested. The cylindrical nanorobot (diameter of 14 nm and length of 48 nm) with a switchable flap, is able to respond to an external stimulus and reacts by a physical switch from a disarmed to an armed configuration able to deliver a cellular compatible message. In the tested design the robot weapon is a nucleic acid fully contained in the inner of the tube and linked to a single point of the internal face of the flap. Upon actuation the nanorobot moves the flap extracting the nucleic acid that assembles into a hemin/G-quadruplex horseradish peroxidase mimicking DNAzyme catalyzing a colorimetric reaction or chemiluminescence generation. The actuation switch is triggered by an external nucleic acid (target) that interacts with a complementary nucleic acid that is beard externally by the nanorobot (probe). Hybridization of probe and target produces a localized structural change that results in flap opening. The flap movement was studied on a two-dimensional prototype origami using Förster resonance energy transfer and was shown to be triggered by a variety of targets, including natural RNAs. The nanorobot has potential for in vivo biosensing and intelligent delivery of biological activators.*

1. Introduction

Deoxynucleic acid (DNA) proved to be an exceptionally versatile material for the development of synthetic devices for use in biosensing. In a first and most traditional aspect, DNA is used as sensing layer in sensors, exploiting the characteristic specificity of the Watson-Crick pairing. Sensors that use nucleic acid as the probe molecule have been studied for at least twenty years and are now broadly used.[1] The reason of their success lies in the ease in the production of synthetic sequences as well as in the ability to determine the potential specificity in silico prior to the actual synthesis and test of the probe. In a second aspect, DNA proved to be an ideal structural material

Dr. E. Torelli, Dr. C. Polano, Prof. G. Firrao
Department of Agricultural
and Environmental Sciences
University of Udine
via delle Scienze 206
33100 Udine, Italy
E-mail: firrao@uniud.it
Dr. M. Marini,[+] Dr. A. Scarpellini
Italian Institute of Technology (IIT)
via Morego 30, 16163 Genova, Italy
[+]Present address: King Abdullah University of Science and Technology
Physical Science & Engineering Division, Kingdom of Saudi Arabia

Dr. S. Palmano
Institute of Plant Virology (IVV)
National Research Council
Strada delle Cacce 73
10135 Torino, Italy
Dr. L. Piantanida, Dr. M. Lazzarino
IOM-CNR National Laboratory TASC, Basovizza
34149 Trieste, Italy

DOI: 10.1002/smll.201400245

for the construction of self assembled, very small objects. One of the most important development in structural DNA nanotechnology has been the use of a scaffold strand and hundreds of short staple strands for the assembly of two-dimensional (2D)[2–4] and three-dimensional (3D)[5–9] DNA origami objects. Several of these DNA-directed assemblies have led to unique and improved functional properties.[10–12] For example, a relevant application of DNA origami concerning label free, ultrasensitive mRNA detection in solution was reported by Ke and co-workers.[13] In their system, on a rectangular-shaped DNA origami, staple strands were elongated with ssDNA overhangs complementary to specific RNA targets; upon ssDNA hybridization with specific mRNAs, the resulting local protrudings were imaged by atomic force microscopy (AFM). Also Seeman and co-workers[14] designed a DNA origami as a molecular chip to detect single nucleotide polymorphisms, further demonstrating the potential of DNA nanostructures for biological sensing applications.[15] In a different approach, a DNA-origami actuator capable of autonomous internal motion was used to detect the presence of a target monitoring the conformation changes by measure of Förster resonance energy transfer (FRET).[4] A third aspect of the use of nucleic acids in biosensing, that has only more recently started to be investigated, concerns the identification through in vitro selection from random libraries of nucleic acid, named DNAzymes, that can catalyze chemical reactions.[16] For example the hemin/G-quadruplex horseradish peroxidase (HRP)-mimicking DNAzyme catalyzes the H_2O_2-mediated oxidation of 2,2′-azinobis-(3-ethylbenzthiazoline-6-sulfonic acid), $ABTS^{2-}$ or the oxidation of luminol by H_2O_2 to yield chemiluminescence.[17,18] Considering the advantages of good stability and easy synthesis, DNAzymes are receiving growing interest in the transduction of biosensing events. Several DNAzyme-based sensors have been reported for the detection of metal ions such as Cu^{2+}, Pb^{2+}, UO_2^{2+} or of aptamer complexes.[19–25] In this work we report the construction of a nano-object made exclusively of DNA, which exploits all three aspects listed above: it is a DNA origami in structure that, when triggered by a specific hybridization event, translates the signal through the activity of a DNAzyme. The nano-object presented exploits a fourth aspect of DNA, as the single to double helix transition is used as fuel to produce a change in the object conformation.

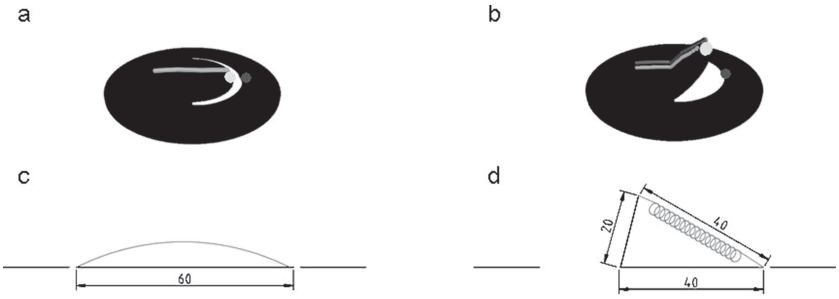

Figure 1. Schematic model of the 2D DNA nanostructure. As represented, the 2D DNA origami has a switchable flap. (a) Upper view of a closed 2D DNA origami (black) with a noncomplemented single stranded probe (pale gray), fluorophore (white dot) and a quencher (gray dot). (b) Upper view of an actuated 2D DNA origami; the probe is hybridized to a complementary target (dark gray) and the distance between fluorophore and quencher increases. (c) Distance (in nm) between the two points on the DNA origami (black) linked by the linear probe molecule (gray). (d) Estimated length of the double helix (gray) and flap opening angle of the DNA origami (black) after probe/target hybridization (length expressed in nm).

2. Results and Discussion

2.1. Rationale

The aim of this work was to build a nanorobot with the ability to carry out a duty when instructed by a molecular signal, typically undergoing a physical change in its structure upon reception of the signal. To obtain the structural modification we used the approach developed by Marini and co-workers,[4] with modifications. In our previous work, a single stranded DNA (probe) linked at its ends to two distant points of a planar DNA origami was hybridized to a hairpin DNA, thus bringing its ends into proximity and consequently driving a deformation of the linked structure. In order to widen the applicability of the method to any possible linear (non hairpin) target, we modified the system so that the movement is fueled by the reduction of distances between the probe ends due to the coiling of the DNA when double stranded formation occurred. To test the approach we first developed a 100 nm planar DNA origami with a prototype flap (**Figure 1**a, b–c and d) and characterized the flap movement with different targets using FRET. Subsequently we developed a 3D cylindrical DNA origami (nanorobot) of a minimal dimension (14 nm x 14 nm x 48 nm) but sufficiently large to host single stranded DNA in its lumen and equipped it with a movable flap (**Figure 2**a). In such a prototype, the actuation of the flap using an external target allows the exposure of the internal ss-DNA, that folds into an active DNAzyme (Figure 2b and c).

2.2. Flap Movement Development Prototype

A planar DNA object with a moving flap was designed according to Figure 1a and b. The DNA origami was obtained by modification of a previous project[4] with the substitution of some staples oligonucleotides as detailed in the supplementary material (Table S1, Supporting Information). According to the design, the moving flap length was about 20 nm, its distal end point is linked to the origami, for movement control, by a 120 nts single stranded DNA (named probe). As shown in Figure 1a and c, the distance between the two points linked by the linear probe molecule, one on the top side of the flap end and the other on the surface of the origami, was 60 nm.

The DNA object was successfully self-assembled in one-pot reaction and characterized by agarose gel electrophoresis, atomic force microscopy (AFM) and transmission electron

small 2014,
DOI: 10.1002/smll.201400245

NANO MICRO small

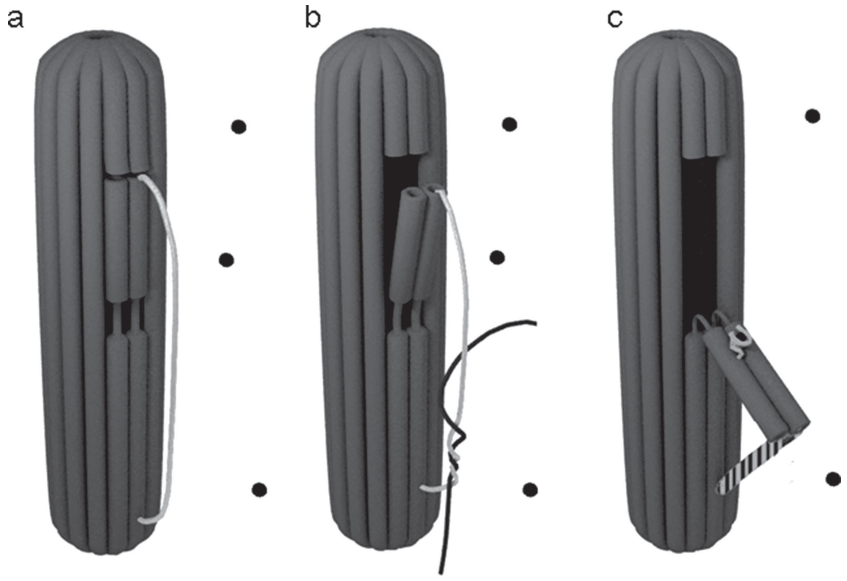

Figure 2. Schematic model of the 3D DNA origami nanorobot with a switchable flap. (a) Closed 3D DNA origami (gray) with the unreacted probe (white). (b) The 3D DNA origami during the hybridization probe (white)/target (black). (c) Actuated 3D DNA origami armed with hemin/G-quadruplex DNAzyme complex: when the probe (white) fully hybridized to target (black), the flap opened and a DNAzyme (pale gray) was pulled out of the cylinder and exposed to hemin (black).

microscopy (TEM) after positive staining. The synthesis resulted in a stable well-folded construct, that migrated during electrophoresis as a distinct band well separated from non-integrated staple strands (Figure S1, Supporting Information).

Structural information about the two dimensional DNA-origami was gained with liquid phase atomic force microscopy that directly revealed the formation of well formed and mainly isolated DNA origami nano-objects with an average diameter of 98 ± 4 nm and average height measured on the external part of disk of 1.8 ± 0.2 nm (**Figure 3**b and c).

TEM imaging showed well formed circular constructs with dimensions smaller than those expected, coherently with previously reported observations.[26] The disk diameter estimated by positive staining was of 83 ± 7 nm (Figure 3a).

In order to control the flap motion of the DNA origami, a target ssDNA (perfectly complementary in sequence to the probe) was added to the solution and hybridized to the probe. The double stranded (ds) DNA formation originated a double helix of an estimated length of 40 nm (Figure 1d). Since the two probe ends were anchored at a distance of 60 nm, this hybridization caused a tensile force that induced a flap motion (Figure 1b and d).

The flap movement process could be monitored by microscopy: AFM and TEM images clearly revealed a hole within the circular DNA origami due to the flap motion, as reported in **Figure 4**. Moreover, as drafted in Figure 1a and b, with the origami in the rest state, a 6′-FAM fluorophore placed at the top of the flap and a BHQ-1 quencher placed on the non moving part of the origami within the Förster radium distance (≈1 nm) are expected to produce a fluorescent signal of low intensity at the FAM emission wavelength. After target to probe hybridization and subsequent flap movement the fluorescent signal intensity is expected to increase. Fluorescent changes were actually obtained using various target/probe combinations, as detailed below.

2.3. Controlling Flap Movement with Synthetic DNA and Natural Virus RNA

The histograms shown in the three panels of **Figure 5** report the results obtained in experiments of actuation of the flap movement of the 2D origami with several different target nucleic acids, including the native RNAs extracted from infected plants using fast processing extraction methods used in routine diagnostics. No variation in fluorescence intensity was recorded when a non target nucleic acid was added to the origami solution, including non target synthetic oligonucleotides and nucleic acids extracted from healthy plants or plants infected with non target viruses (bars a, c, e, g, and h in each histogram of Figure 5). On the contrary, when the flap was moved due to the addition of a probe complementary to the target, the consequent FRET couple

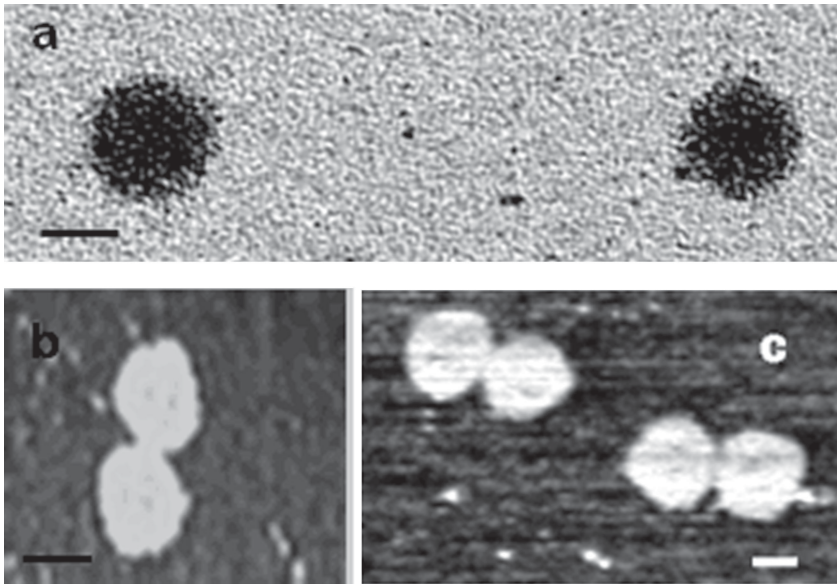

Figure 3. TEM (a) and AFM (b, c) imaging of well formed DNA origami structures. Scale bars: 50 nm.

DOI: 10.1002/smll.201400245

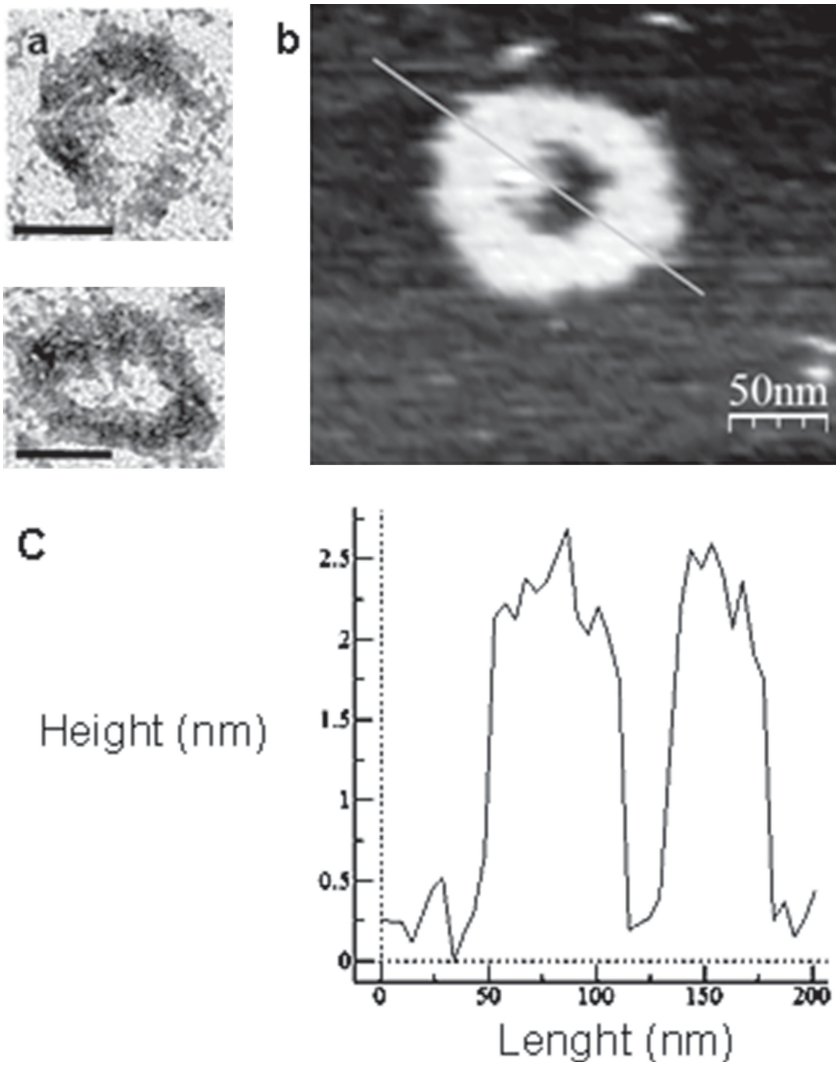

Figure 4. TEM images (a) and AFM image (b) of well formed DNA origami disks with actuated flap and related height profile (c). Scale bars panel a: 50 nm.

separation resulted in an appreciable increase in the fluorescence signal intensity. Significant variations in fluorescence intensities were obtained with synthetic linear and clamp DNAs complementary to the probe (Figure 5, bars b and d) and also with RNAs extracted from plant infected with target viruses (Figure 5, bar f). Thus, origami having as probes DNA sequences designed to be complementary to the nucleocapsid genes of diverse viruses such as TMV (Tobacco Mosaic Virus), TSWV (Tomato Spotted Wilt Virus), and IYSV (Iris Yellow Spot Virus), reacted specifically with the respectively correct targets, proving that this versatile system does not require ad hoc designed synthetic targets for actuation, but can be easily adapted to perform detection of specific natural, unlabeled nucleic acids, even in mixtures with an excess of unrelated nucleic acids. The specificity, evidenced by the clear cut discrimination between the signals produced by the detection of target and non-target viruses, as well as the sensitivity (the amount, used in each experiment was 30 ng of total, including host and virus, RNA) were promising for the use of methods based on this principle in diagnostics.

The advantageous feature of a detection system based on conformational changes of a DNAorigami platform is its potential for integration of the detection step with a reporting system. Below we report the proof of concept for an integrated system that exploits DNA origami conformational changes associated with single molecule detection to control an enzyme-like reporting activity, without the need of an external transducer.

2.4. Implementing Flap Movement on a Nanorobot

The flap devoloped above was reduced in size and included in a 3D origami of cylindrical shape according to Figure 2a,b and c. Detail on the caDNAno project, the list of oligonucleotides used for its synthesis and CanDo fluctuation movie (viewed from both sides, with and without flap, respectively) are provided as supporting information (Figure S2, Table S2, Movie1 and Movie2). The designed nanorobot had estimated dimensions of 14 nm × 14 nm × 48 nm. The volume of the inside cavity (8 nm × 8 nm × 44 nm) was estimated to be 3 zeptoliters. The flap dimensions were 9 nm × 5 nm, and the distance between the anchored probe tails was 28 nm. Since this nano-object was designed to be of minimal dimensions, the M13mp18 ssDNA used as scaffold strand was pre processed with enzymatic digestion and only one fragment was used for the folding of the origami. After folding, the nano-object was purified using agarose gel electrophoresis followed by extraction, desalting and concentration steps (Figure S3 and Figure S4 Supporting Information). The overall efficiency of the synthesis and purification process was estimated to be 21% by measurement of the optical density of the recovered DNA nanostructure that, according to subsequent agarose gel and AFM visualization, resulted intact and without excess staple strand contamination. Recently, rate-zonal centrifugation was reported as an efficient method to obtain large amounts of DNA origami.[27] Such a purification method would permit higher recovery yield if large-scale DNA nanorobots had to be required for biosensing.

TEM and AFM images (**Figure 6** and **7**) confirmed the correct formation of the 3D DNA origami and the average value of the nano-object was calculated on 1500 nanostructures. Their length resulted 55 ± 9 with AFM and 40 ± 7 nm with TEM, i.e. smaller than predicted, in agreement with previous observations of Sander and Golas[26] who visualized a DNA box using conventional negative staining and TEM instead of AFM and cryo-EM used by Andersen et al.[5] and reported that negative staining and air drying resulted in an apparent shrinkage of the hollow DNA box.

small 2014,
DOI: 10.1002/smll.201400245

NANO MICRO small

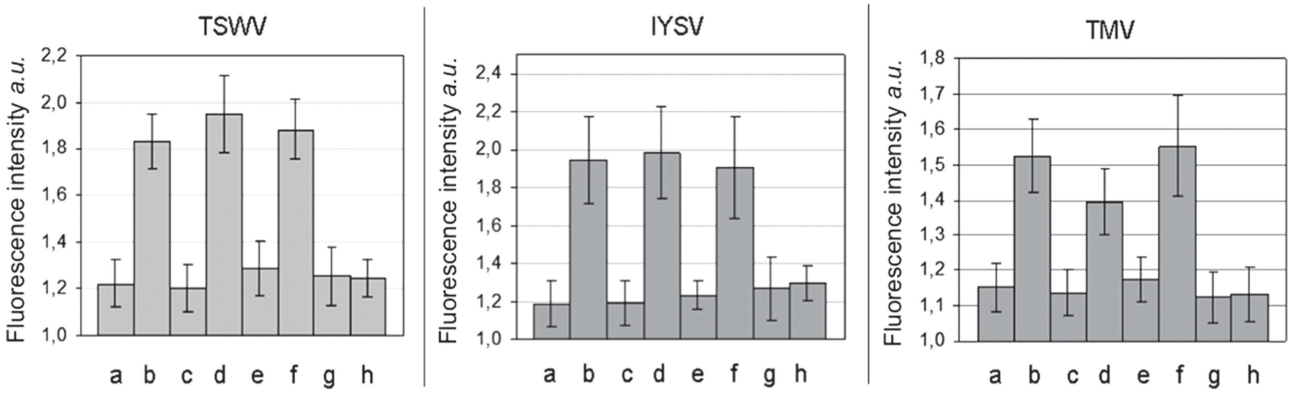

Figure 5. Validation of the DNA-origami system with viral RNAs from *Nicotiana benthamiana* inoculated with Tomato Spotted Wilt Virus (TSWV), Iris Yellow Spot Virus (IYSV) and Tobacco Mosaic Virus (TMV). In all the histograms the fluorescence intensities (expressed in arbitrary units) emitted by a 3.2 nM solution of DNA-origami as synthesized (a), actuated with a complementary clamp target (b) or after the addition of a linear synthetic target (d) or of the viral RNA of interest (f) are reported together with the negative controls after the addition of a non complementary clamp target (c), linear target (e), viral RNA (g) and plant RNA (h). Each bar is the average of at least 20 independent measurements.

The DNA nanorobot was assembled, purified and subjected to FRET measurements to confirm the flap opening following target addition. In the absence of the target (closed state), the fluorophore 6'-FAM and the quencher BHQ-1 were in close proximity resulting in a low FRET emission, as demonstrated by a low fluorescent signal intensity. A significant increase of the fluorescent intensity could be detected, demonstrating flap motion determining the consequent FRET pair separation, after 1 h incubation at room temperature in the presence of the target (**Figure 8**).

2.5. Operational Characterization of the Nanorobot

Recent studies showed that 3D DNA nanostructures can be dynamically manipulated by external DNA sequences or proteins. DNA locks and DNA keys[5,9] or antigen keys[8] have been used to control the opening of DNA nanocontainers which may act as drug delivery vehicles. In particular, Douglas et al.[8] described an autonomous DNA nanorobot capable of transporting and delivering molecular payloads to a specific location.

Here, we integrated a DNAzyme cargo in the cylindrical DNA origami equipped with a flap described above. The cargo was the 20 nts long hemin-binding sequence PS2.M[17] that was included into the oligonucleotide 22[95]bis (Table S2, Supporting Information) origami self-assembly. As a result, this 84 nts long oligonucleotide protruded for about 20 nts toward the inner of the cylinder in the non hybridized configuration. After the addition of a DNA target (the TMV sequence was used for the purpose) and movement of the flap in an open position, the PS2.M protruding stretch was pulled out of the cylinder and exposed to the external solution. The incorporation of hemin via the formation of intramolecular guanine quadruplexes defined a cofactor-utilizing nucleic acid that catalyzes oxidative chemistries.

To confirm the occurence of the process, we used a colorimetric assay based on the catalyzed oxidation of $ABTS^{2-}$ by H_2O_2 and an assay based on the generation of chemiluminescence in the presence of luminol/H_2O_2. As shown in **Figure 9**, the activation of flap movement with 20 pmol of target DNA could be detected with the colorimetric assay, although control experiments revealed some residual activity catalized by hemin in the absence of DNA. This noise was lower in the chemiluminescent assay (**Figure 10**), that allowed to lower the detection limit to 12 pmol and also increase the signal to noise ratio. This is a first example of an integration of a hidden DNAzyme in a three dimensional DNA origami, that provided an obvious operational advantage as compared with previously reported detection systems based on DNA origami relying on the analysis by AFM to reveal structural changes.[13,28] Other examples of use of DNAzymes with DNA origami have been reported by Lund et al.[29] and by Johnson-Buck et al.;[30] in these cases the tasks performed by the DNAzymes were related to the functional activation of the origami to permit molecular spider walk or to show probe-binding patterns in points accumulation for imaging in nanoscale topography (PAINT).

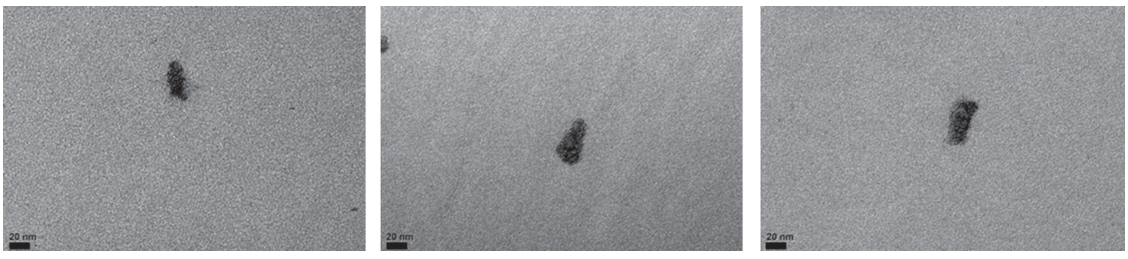

Figure 6. Positive-staining TEM images of three dimensional DNA nanorobot.

DOI: 10.1002/smll.201400245

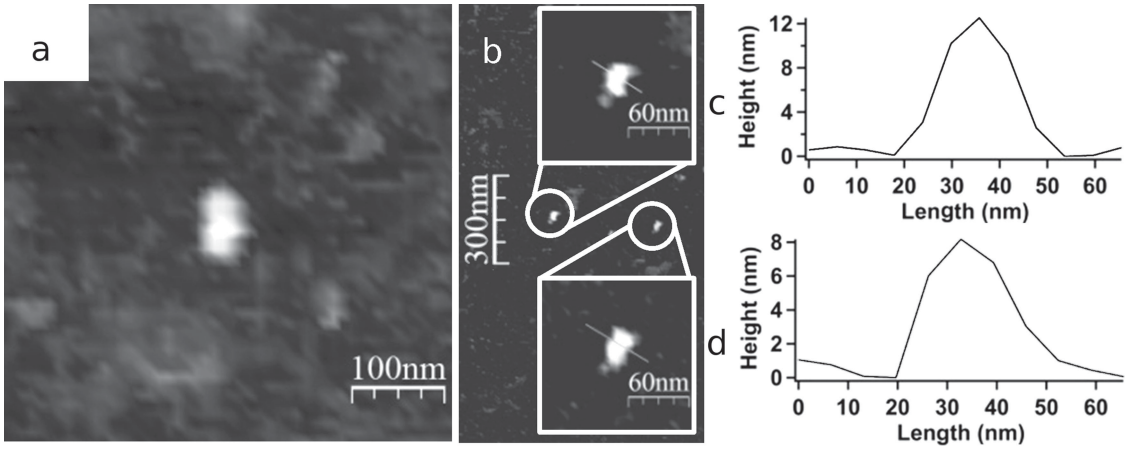

Figure 7. (a, b) AFM image of the nanorobot structure. (c, d) Height profile analysis of two different structures underlined in the zoomed insets of image (b): the profile (c) is referred to the top inset, the profile (d) is referred to the bottom inset. The maximum height difference could be attributed to the pushing effect of the AFM tip.

In summary, we have demonstrated the versatility and potential in biosensing of an origami based nanoactuation mechanism and then we designed, synthesized, imaged and operated a three dimensional DNA nanorobot capable of a switch in response to an external signal using this nanoactuation method. In the presence of a small amount of target DNA the robot moves a flap promoting the exposition of its cargo DNA and the self-assembly of stable hemin/G-quadruplex DNAzyme. The nanoactuation mechanism that controls flap movement is similar to a molecular spring, fueled by DNA coiling, that actively pull the flap and it is therefore well distinct from other published box opening mechanisms[5,8] that simply rely on the removal of a lock and do not actively drive the opening movement.

Another peculiarity of the system presented here is the integration of a DNA cargo in the construction of the origami and its containment in an inactive state within its body. Thus, this self-assembled robot, when instructed, gets armed by the further self assembly step of a DNAzyme upon exposition of a previously hidden sequence. This strategy simplify the loading process, granting for high efficiency and allowing reduction of the final dimensions of the container to a minimum.

The switching between a hidden/exposed cargo conformation was exemplified in this work with a DNAzyme, but it can easily be adapted to allow the controlled delivery of nucleic acid coded cellular messages, such as microRNAs or ribozymes, that can be made available for interaction with the environment only after activation of the flap opening.

3. Conclusion

DNA sensors are of particular interest since DNA analysis plays a crucial role in a wide range of areas including monitoring of infectious agents, analysis of forensic samples and detection of bioterrorism agents.[31] The present study has demonstrated the use of the DNA origami technology for the construction of a nanorobot able to detect picomol amounts of a DNA target and reveal it using a DNAzyme as the biocatalytic label.

To our knowledge, this is the smallest size 3D DNA-origami characterized by a controllable lid and capable of accommodating a functional cargo in its lumen. Smaller 3D DNA nanostructures have been reported, such as the DNA tetrahedron developed by Goodman et al.,;[32] This DNA polyhedral structure (maximum dimension ≈ 7 nm) was capable of entering live mammalian cells:[33] however DNA tetrahedra did not combine closed surfaces with a hollow cavity with the potential capacity to accommodate a cargo.[9] As far as the nanorobot presented here is concerned, the lumen is large enough to accommodate a single stranded nucleic acid, while the nano-object is small enough to be entirely contained within the capsid of viruses.[34] This work therefore opens perspectives for the construction of nanorobots that can be hosted within cellular delivery vectors and can host, concurrently, selectively accessible molecular payloads in their internal cavity.

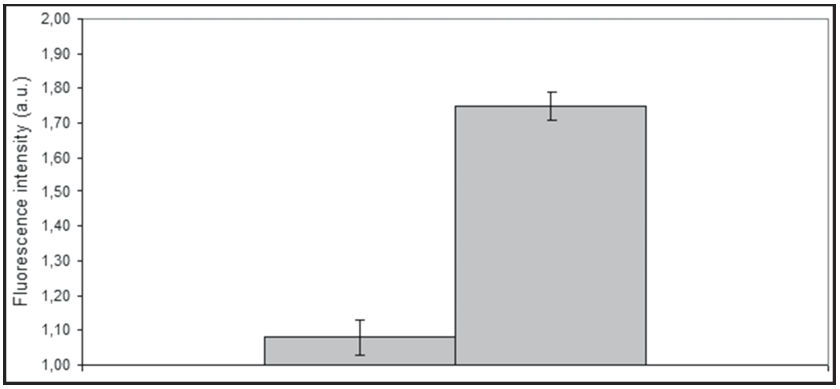

Figure 8. FRET measurements of the close DNA nanorobot with (b) and without (a) the addition of the TMV target sequence (fluorescence intensity is expressed in arbitrary units).

small 2014,
DOI: 10.1002/smll.201400245

NANO MICRO small

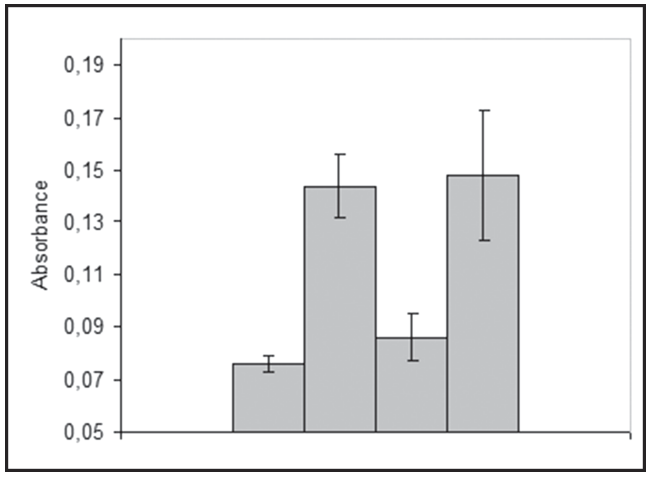

Figure 9. Absorbance value of the background (a), DNAzyme (8 nM; b), hemin/G-quadruplex DNAzyme complex in the absence of the target sequence (closed DNA nanorobot, c) or in the presence of the target sequence (actuated DNA nanorobot, d).

4. Experimental Section

Materials and reagents: Hemin was purchased from Porphyrin Products (Logan, UT) and used without other purification. A hemin stock solution (50 mM) was prepared in DMSO and stored in the dark at −20 °C. All other chemicals were purchased from Sigma-Aldrich (Germany). All oligonucleotides were standard purified and resuspended in ultrapure water to give stock solutions of 100 μM. M13mp18 and *Xmn*I enzyme were purchased respectively from Bayou Biolabs, LA, USA and NewEngland Biolabs, Ipswich, MA.

Scaffold strand design: The DNA origami objects were designed using the square-lattice version of the caDNAno software from Douglas et al. (2009).[6] To obtain the 2D circular shape, the entire single-stranded circular DNA of the M13mp18 viral genome (7249 nts) was used as scaffold sequence input. To design and assembly the 3D origami object, the single-stranded M13mp18 genome was digested at the two *Xmn*I restriction sites after the hybridization of ssDNA with *Xmn*I cut-site oligonucleotides: the resulting 2289 nts scaffold strand was incorporated into the 3D DNA origami structure. The computational tool CanDo was used to compute 3D DNA origami shape based on caDNAno design file.[35,36] DNA origami folding paths and oligonucleotides sequences are reported in Supplementary Information.

DNA actuation design: The probe and target sequences were drawn using the software Bioedit 7.2.0.[37] evaluating the possible secondary structures and the thermodynamic details with the mfold web server.[38] To investigate the correct hybridization of the target/probe complex, the complementary strands were preliminarily annealed in equimolar proportion in a saline 1 μM solution containing 1× TAEM buffer. The solutions were heated at the denaturing temperature of 95 °C for two minutes to open undesired DNA hairpin or secondary structures and then cooled at room temperature. When used for actuation, the target was added in a 10:1 concentration relative to the probe; the probe was added in the origami mix solution in a 1:1 concentration relative to the DNA staples.

2D DNA assembly and Purification: The 2D DNA origami was produced by mixing 1.6 nM of circular M13mp18 DNA and 16 nM of each staple strands (218 oligonucleotides) in 100 μL of TAEM (10x TAEM solution is 125 mM $MgCl_2$, 400 mM Tris-HCl, 10 mM EDTA pH 8.0, 20 mM NaCl). The mixture was subjected to a thermal-annealing ramp and the folded constructs were purified from staple strands excess, as reported by Marini and co-workers.[4]

3D DNA assembly and Purification: The ss M13mp18 (21 nM) was mixed with the cut-site oligonucleotides (2.1 mM) in the restriction buffer 4, heated to 95 °C for 3 minutes and allowed to cool to 37 °C. The solution was digested with *Xmn*I enzyme at 37 °C for 6 hours. After heat deactivation of the enzyme, the assembly reactions were performed in TAEM containing the cut scaffold, the 82 staple strands (each at 0.19 mM concentration) and the probe ssDNA (4.5 nM).[4] The mixture was annealed from 95 to 25 °C at a rate of 0.01 °C/s ramp. The solution was concentrated using an Amicon Ultra 0.5 mL 100 kDa centrifugal filters (Millipore, Massachusetts): capped Amicon Ultra were centrifuged at 10 000 g for 6 min at 15 °C. Concentrated samples were eluted spinning the inverted filters in a clean vial at 300 g for 10 min at 15 °C and run in a 0.7% agarose gel in 1x TAE at 75 V for 90 min. After running, the desired bands were excised, and the gel slice placed into a filter cup (Quantum Prep™ Freeze'n Squeeze Gel extraction Spin Columns, Biorad Laboratoires, CA): the filter cup was put at −20 °C for 5 min, then removed and centrifuged at 13 000 g for 3 minutes. To remove contaminants and concentrate sample, the DNA origami solution was filled into one Amicon Ultra centrifugal filter and centrifugated three times at 10 000 g for 6 min at 15 °C. Between every centifugation step, the flowthrough is removed and the filter is refilled with 400 μL of 10 mM Tris-HCl buffer (pH 7.4) containing 10 mM KCl, 100 nM NaCl and 0.002% (v/v) Triton X-100.[39] To recover the DNA origami sample, the filter was turned upside down and centrifuged once more at 300 g for 10 min at 15 °C. ImageJ was used for gel image analysis to estimate yield of purification.[40]

Nucleic Acids Visualization: Folded and purified DNA-origami were electrophoresed on 0.7% (w/v) agarose gel (Pronadisa): gels were previously added of 0.5× Gel Red™ nucleic acid stain (Biotium, Hayward, CA) and run in 1× TAE (for 200 mL of a 50× buffer

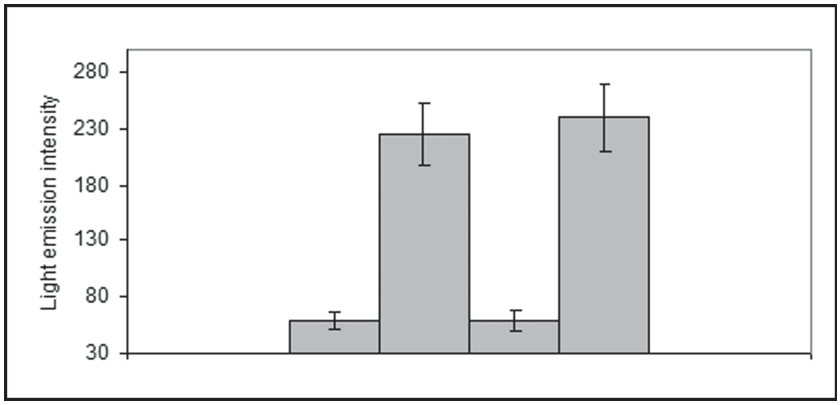

Figure 10. Light emission intensity (expressed in pixel units) of the background (a), DNAzyme (16 nM; b), hemin/G-quadruplex DNAzyme complex in the absence of the target sequence (closed DNA nanorobot, c) or in the presence of the target sequence (actuated DNA nanorobot, d).

DOI: 10.1002/smll.201400245

solution: 400 mM Tris-HCl, 11.42 mL acetic acid, 20 mL EDTA 0.5 M, pH 8.0) at 75 V for 90 minutes and then visualized and photographed under UV light (VisionWorksLS Image Acquisition and Analysis Software, UVP, CA). The Gene Ruler 1 kb DNA ladder (Fisher Scientific, Italy) was used as a molecular weigth marker.

TEM imaging: For TEM imaging 10 μL of the samples were adsorbed for 3 minutes on carbon-coated copper grids and imaged with a JEOL JEM 1011 transmission electron microscope (Tokyo, Japan) operating at 100 kV. The samples were stained for 2 minutes with a 2% uranyl acetate solution and washed in milliQ water for three times. TEM images were analyzed using the software Gatan Digital Micrograph or ImageJ.[40]

AFM imaging: Samples were dispersed on freshly cleaved mica in 10x TAEM buffer to allow the presence of bivalent cations as Mg^{2+} to ensure the adhesion of the negative charged DNA origami structures on the negative mica surface. Samples were let sediment for 5 minutes in a humid chamber to avoid the drying of the sample. The 2D DNA origami images have been obtained using a JPK Nanowizard II atomic force microscope using Bruker probes (Bruker Italia S.r.l., Milano, Italy). The 3D DNA origami images have been recorded using either a JPK Nanowizard II, a VEECO Multimode with Nanoscope V control or an Asylum MFP3D AFM system. We used Olympus OMCL-TR400PSA tips with a force constant of 0.08 N/m and a resonance frequency of 34kHz, in air. All the AFM measurements where operated in liquid in tapping mode. Image analysis were performed using the software Gwyddion.[41]

Validation with real samples: All test plants were grown in sterilized soil under insect-free conditions. Viruses and phytoplasma strains used belong to IVV collection. Original freeze-dried plant material stored at −20 °C of Tobacco Mosaic Virus (TMV- IFA9strain), Tomato Spotted Wilt Virus (TSWV- P105 strain) and Iris Yellow Spot Virus (IYSV- Cip6 strain), were mechanically inoculated on *Nicotiana benthamiana*. Freeze-dried leaf tissue was homogenized (1/5 w/v) with 50 mM phosphate buffer pH 7 containing 1 mM Na-EDTA, 5 mM Na-DIECA, 5 mM Na-thioglycolate and 50 mg/mL activated charcoal. Inoculums, mortars and buffer were cooled on ice before and during inoculation. Total RNA from 0.1 g of symptomatic leaves of *N. bentamiana* (viruses) was extracted using RNeasy Plant Mini Kit (Qiagen, Hilden, Germany) according to the manufactures instruction and quantified with Nanodrop 1000 spectrophotometer.

Colorimetric assays: Opening of the closed 3D DNA origami was induced using 0.5 μM nucleic acid target and allowed to react for 1 hour (reaction volume: 37.5 μL). To bring the volume to 200 μL, 10 mM Tris-HCl buffer (pH 7.4) containing 10 mM KCl, 100 mM NaCl and 0.002% (v/v) Triton X-100 was added. In order to ensure the formation and availability of G-quadruplex structures through the opening of the origami, the mixture was heated at 40 °C for 3 minutes, and then incubated at 25 °C for 30 minutes. To this solution was added 2 mM ATP and the solution was allowed to incubate at 25 °C for 30 minutes. Hemin (0.2 μM) was added to the mixture. The reaction mixture was held for another 1 h at 25 °C, and then 0.5 mM of ABTS and 1.2 mM of H_2O_2 were added, as reported by Kong group.[39] DNA origami configuration change was monitored by absorbance measurements at 410 nm using a microplate reader (Dynatech Microplate Reader Model MR 5000, Dynex technologies, USA) after the reaction had run for 55 minutes.

Chemiluminescence assays: Opening of the closed 3D DNA origami was induced using 0.5 μM nucleic acid target and allowed to react for 1 hour (reaction volume: 21.5 μL). As reported above, the mixture was heated at 40 °C for 3 minutes, and then incubated at 25 °C for 30 minutes. Then, hemin was added and incubated for 1 h at 25 °C to form the respective hemin/G-quadruplex structures. The assays were performed in a solution containing 0.96 μM hemin, 0.5 mM luminol and 30 mM H_2O_2. Briefly, the DNA origami solution and 3.3 μL of 5 mM luminol were added to a micro cuvette. Then 10 μL of H_2O_2 stock solution (98 mM) was quickly added, as reported by Liu et al.[42] DNA origami opening was measured immediately with a CCD detector (model AP47p, Apogee) analyzing the light emission intensity.

FRET System: DNA origami motion was directly monitored with a CCD detector (model AP47p, Apogee) mounted on a fluorescence microscopy (Leitz Orthoplan), analyzing 12 μL of sample illuminated with an exciting 470 nm blue emission and a 517–540 nm filter.

Supporting Information

Supporting Information is available from the Wiley Online Library or from the author.

Acknowledgement

This work was supported by the Italian Ministery of University and Research through the program PRIN, project 2008F2-F82F. Tomaso Firrao is gratefully acknowledged for providing the drawings of the nanorobot.

[1] P. Arora, A. Sindhu, N. Dilbaghi, A. Chaudhury, *Biosens. Bioelectron.* **2011**, *28*, 1.
[2] P. W. K. Rothemund, *Nature* **2006**, *440*, 297.
[3] M. Endo, T. Sugita, A. Rajendran, Y. Katsuda, T. Emura, K. Hidaka, H. Sugiyama, *Chem. Commun.* **2011**, *47*, 3213.
[4] M. Marini, L. Piantanida, R. Musetti, A. Bek, M. Dong, F. Besenbacher, M. Lazzarino, G. Firrao, *Nano Lett.* **2011**, *11*, 5449.
[5] E. S. Andersen, M. Dong, M. M. Nielsen, K. Jahn, R. Subramani, W. Mamdouh, M. M. Golas, B. Sander, H. Stark, C. L. P. Oliveira, J. S. Pedersen, V. Birkedal, F. Besenbacher, K. V. Gothelf, J. Kjems, *Nature* **2009**, *459*, 73.
[6] S. M. Douglas, H. Dietz, T. Liedl, B. Hogberg, F. Graf, W. M. Shih, *Nature* **2009**, *459*, 414.
[7] V. J. Schüller, S. Heidegger, N. Sandholzer, P. C. Nickels, N. A. Suhartha, S. Endres, C. Bourquin, T. Liedl, *ACS Nano* **2011**, *5*, 9696.
[8] S. M. Douglas, I. Bachelet, G. M. Church, *Science* **2012**, *335*, 831.
[9] R. M. Zadegan, M. D. E. Jepsen, K. E. Thomsen, A. H. Okholm, D. H. Schaffert, S. E. Andersen, V. Birkedal, J. Kjems, *ACS Nano* **2012**, *6*, 10050.
[10] A. V. Pinheiro, D. Han, W. M. Shih, H. Yan, *Nat. Nanotechnol.* **2011**, *6*, 763.
[11] C. Song, Z. G. Wang, B. Ding, *Small* **2013**, *9*, 2382.
[12] Z. G. Wang, C. Song, B. Ding, *Small* **2013**, *9*, 2210.
[13] Y. Ke, S. Linsday, Y. Chang, Y. Liu, H. Yan, *Science* **2008**, *319*, 180.

DOI: 10.1002/smll.201400245

[14] H. K. Subramanian, B. Chakraborty, R. Sha, N. C. Seeman, *Nano Lett.* **2011**, *11*, 910.
[15] H. Li, T. H. LaBean, K. W. Leong, *Interface Focus* **2011**, *1*, 702.
[16] A. D. Ellington, J. W. Szostak, *Nature* **1990**, *346*, 818.
[17] P. Travascio, Y. Li, D. Sen, *Chem. Biol.* **1998**, *5*, 505.
[18] Y. Xiao, V. Pavlov, R. Gill, T. Bourenko, I. Willner, *ChemBioChem* **2004**, *5*, 374.
[19] J. Liu, Y. Lu, *Chem. Commun.* **2007**, *46*, 4872.
[20] J. Liu, A. Brown, X. Meng, D. Cropek, J. Istok, D. Watson, Y. Lu, *PNAS* **2007**, *104*, 2056.
[21] J. Elbaz, B. Shlyahovsky, I. Willner, *Chem. Comm.* **2008**, *13*, 1569.
[22] B. C. Yin, B. C. Ye, W. Tan, H. Wang, C. C. Xie, *J. Am. Chem. Soc.* **2009**, *131*, 14624.
[23] G. Pelossof, R. Tel-Vered, I. Willner, *Anal. Chem.* **2012**, *84*, 3703.
[24] T. Li, E. Wang, S. Dong, *Chem. Commun.* **2008**, *31*, 3654.
[25] T. Li, E. Wang, S. Dong, *Chem. Commun.* **2008**, *43*, 5520.
[26] B. Sander, M. M. Golas, *Microsc. Res. Technol.* **2011**, *74*, 642.
[27] C. Lin, S. D. Perrautl, M. Kwak, F. Graf, W. M. Shih, *Nucleic Acids Res.* **2013**, *41*, e40.
[28] A. Kuzuya, Y. Sakai, T. Yamazaki, Y. Xu, M. Komiyama, *Nat. Commun.* **2011**, *2*, 449.
[29] K. Lund, A. J. Manzo, N. Dabby, N. Michelotti, A. Johnson-Buck, J. Nangreave, S. Taylor, R. Pei, M. N. Stojanovic, N. G. Walter, E. Winfree, H. Yan, *Nature* **2010**, *465*, 206.
[30] A. Johnson-Buck, J. Nangreave, D.-N. Kim, M. Bathe, H. Yan, *Nano Lett.* **2013**, *13*, 728.
[31] D. Li, S. Song, C. Fan, *Acc. Chem. Res.* **2010**, *43*, 631.
[32] R. P. Goodman, I. A. T. Schaap, C. F. Tardin, C. M. Erben, R. M. Berry, C. F. Schmidt, A. J. Tuberfield, *Science* **2005**, *310*, 1661.
[33] A. S. Walsh, H. Yin, C. M. Erben, M. J. A. Wood, A. J. Tuberfield, *ACS Nano* **2011**, *5*, 5427.
[34] D. Cardinale, N. Carette, T. Micron, *Trends Biotechnol.* **2012**, *30*, 369.
[35] S. M. Douglas, A. H. Marblestone, S. Teerapittayanon, A. Vazquez, G. M. Church, W. M. Shih, *Nucleic Acids Res.* **2009**, *37*, 5001.
[36] C. E. Castro, F. Kilchherr, D. N. Kim, E. L. Shiao, T. Wauner, P. Wortmann, M. Bathe, H. Dietz, *Nature* **2011**, *8*, 221.
[37] T. A. Hall, *Nucleic Acids Symp. Ser.* **1999**, *41*, 95.
[38] M. Zuker, *Nucleic Acids Res.* **2003**, *31*, 3406.
[39] D. M. Kong, J. Xu, H. X. Shen, *Anal. Chem.* **2010**, *82*, 6148.
[40] M. D. Abramoff, P. J. Magalhaes, S. J. Ram, *Biophotonics Int.* **2004**, *11*, 36.
[41] D. Nečas, P. Klapetek, *Cent. Eur. J. Phys.* **2012**, *10*, 181.
[42] X. Liu, R. Freeman, E. Golub, I. Willner, *ACS Nano* **2011**, *5*, 7648.

Received: January 28, 2014
Revised: February 26, 2014
Published online: